Molecular Simulations of Aqueous Electrolyte Solubility: 1. The Expanded-Ensemble Osmotic Molecular Dynamics Method for the Solution Phase

Martin Lísal,*,†,‡ William R. Smith,§ and Jiří Kolafa||

E. Hála Laboratory of Thermodynamics, Institute of Chemical Process Fundamentals, Academy of Sciences of the Czech Republic, 165 02 Prague 6, Czech Republic, Department of Physics, J. E. Purkyně University, 400 96 Ústí n. Lab., Czech Republic, Faculty of Science, University of Ontario Institute of Technology, 2000 Simcoe St. N., Oshawa, ON L1H7K4, Canada, and Institute of Physical Chemistry, Prague Institute of Chemical Technology, 166 28 Prague 6, Czech Republic

Received: February 11, 2005; In Final Form: May 4, 2005

We have developed a molecular-level simulation technique called the expanded-ensemble osmotic molecular dynamics (EEOMD) method, for studying electrolyte solution systems. The EEOMD method performs simulations at a fixed number of solvent molecules, pressure, temperature, and overall electrolyte chemical potential. The method combines elements of constant pressure−constant temperature molecular dynamics and expanded-ensemble grand canonical Monte Carlo. The simulated electrolyte solution systems contain, in addition to solvent molecules, full and fractional ions and undissociated electrolyte molecular units. The fractional particles are coupled to the system via a coupling parameter that varies between 0 (no interaction between the fractional particle and the other particles in the system) and 1 (full interaction between the fractional particle and the other particles in the system). The time evolution of the system is governed by the constant pressure−constant temperature equations of motion and accompanied by random changes in the coupling parameter. The coupling-parameter changes are accepted with a probability derived from the expanded-ensemble osmotic partition function corresponding to the prescribed electrolyte chemical potential. The coupling-parameter changes mimic insertion/deletion of particles as in a crude grand canonical Monte Carlo simulation; if the coupling parameter becomes 0, the fractional particles disappear from the system, and as the coupling parameter reaches unity, the fractional particles become full particles. The method is demonstrated for a model of NaCl in water at ambient conditions. To test our approach, we first determine the chemical potential of NaCl in water by the thermodynamic integration technique and by the expanded-ensemble method. Then, we carry out EEOMD simulations for different specified values of the overall NaCl chemical potential and measure the concentration of ions resulting from the simulations. Both computations give consistent results, validating the EEOMD methodology.

1. Introduction

Electrolytes are substances such as sodium chloride (NaCl) or calcium chloride ($CaCl_2$) whose aqueous solutions conduct an electric current. Not all electrolytes conduct current to the same extent, and we distinguish between strong and weak electrolytes. In strong electrolytes such as NaCl, all the atoms essentially completely dissociate in solution into free ions (Na^+ and Cl^-), which are available to conduct the current. In weak electrolytes such as mercury(II) chloride ($HgCl_2$), only a small fraction of the atoms dissociate into free ions ($HgCl^+$, Hg^{2+}, and Cl^-); undissociated molecular units ($HgCl_2$) are the predominant solution solute species.[1]

The accurate prediction of the solubility of electrolytes in solvents is a problem of general interest, because of the role that electrolyte solutions play in industrial applications and biological systems. When considering the solubility of solid electrolytes in solvents, one can view the dissolution process as a reaction or a set of reactions, in which molecules of the pure crystalline electrolyte are decomposed into individual ionic species in the solvent. At saturation, the solid electrolyte may be regarded as a reservoir at constant chemical potential, supplying ions and undissociated molecular units to the solution with which it is in equilibrium. For example, the equilibrium dissolution process in the case of NaCl(s) in water is described by the reaction

$$\mathrm{NaCl(s)} \rightleftharpoons \mathrm{Na^+(aq)} + \mathrm{Cl^-(aq)} \tag{1}$$

and the equilibrium dissolution process in the case of $HgCl_2$(s) in water may be described by the set of reactions

$$\mathrm{HgCl_2(s)} \rightleftharpoons \mathrm{HgCl_2(aq)}$$

$$\mathrm{HgCl_2(s)} \rightleftharpoons \mathrm{HgCl^+(aq)} + \mathrm{Cl^-(aq)}$$

$$\mathrm{HgCl_2(s)} \rightleftharpoons \mathrm{Hg^{2+}(aq)} + 2\mathrm{Cl^-(aq)} \tag{2}$$

The solubility of a solid electrolyte in a solvent is measured by the concentration of the saturated solution in equilibrium with the pure crystalline electrolyte. For example, the solubility of

* Corresponding author. Mailing address: E. Hála Laboratory of Thermodynamics, Institute of Chemical Process Fundamentals, Academy of Sciences of the Czech Republic, Rozvojová 135, 165 02 Prague 6-Suchdol, Czech Republic.

† Academy of Sciences of the Czech Republic.

‡ J. E. Purkyně University.

§ University of Ontario Institute of Technology.

|| Prague Institute of Chemical Technology.

10.1021/jp0507492 CCC: $30.25
Published on Web 06/14/2005

NaCl in water (see eq 1) is determined by the concentration of the Na^+ and Cl^- ions in the solution at which the sum of the chemical potentials for the individual ions, $\mu_{Na^+(aq)}$ and $\mu_{Cl^-(aq)}$, is equal to the chemical potential of crystalline NaCl, $\mu_{NaCl(s)}$, at the same pressure P and temperature T, that is

$$\mu_{Na^+(aq)} + \mu_{Cl^-(aq)} = \mu_{NaCl(s)} \quad \text{at given } (P, T) \qquad (3)$$

The solubility of $HgCl_2$ in water (see eq 2) is measured similarly, as the stoichiometric sum of the concentrations of the Hg-containing ionic and undissociated species.[2]

Molecular-level simulation studies concerning electrolyte solubilities are rather rare. Cui and Harris[3] studied the solubility of NaCl in steam and in supercritical water, and Ferrario et al.[4] simulated the solubility of potassium fluoride (KF) in water at near-ambient conditions. In both works, the electrolyte solubility was calculated indirectly. The authors first evaluated the chemical potential of pure crystalline electrolyte; Cui and Harris calculated $\mu_{NaCl(s)}$ by the quasiharmonic approximation,[5] while Ferrario et al. determined $\mu_{KF(s)}$ by the Frenkel−Ladd thermodynamic integration technique.[6] Then, the authors performed a series of constant pressure−constant temperature simulations for the aqueous electrolyte solution at varying concentration, in which they measured the electrolyte chemical potential in the solution. The solubility was then indirectly determined by finding the equilibrium point of the reaction corresponding to eq 3. Such an indirect determination of the electrolyte solubility is very inefficient and time-consuming; a method capable of directly determining the solubility would greatly facilitate molecular-level-based studies of electrolyte solubilities.

The simulation of electrolyte solutions (especially aqueous electrolyte solutions at ambient conditions) is not an easy task. Traditional Monte Carlo (MC) displacement moves[6,7] become very inefficient because of ion pairing and clustering. Unless special MC multiparticle moves such as dipole and cluster moves[6,8,9] are employed, the molecular dynamics (MD) approach is superior to MC, since MD relies on the collective motions of particles. The simulation of electrolyte chemical potentials in solution (especially at finite concentrations) or the simulation of open (at fixed chemical potential) electrolyte solutions is another formidable task because of the large free-energy differences associated with creation/destruction of ions in the solution. The traditional Widom test-particle-insertion method for measurement of the chemical potential[10] is not feasible.[3] Instead, electrolyte chemical potentials in solution are typically determined by a thermodynamic integration technique[6] or by the expanded-ensemble method.[11−13] The former technique is time-consuming, whereas the latter method requires expertise in the prior determination of balancing factors.

Calculation of electrolyte solubility requires the ability to perform simulations of electrolyte solution systems at a specified chemical potential (open systems). Simulation studies of such electrolyte systems have so far been limited to the restricted primitive model of electrolytes.[8,9,14−16] Orkoulas and Panagiotopoulos[8,9] developed a grand canonical MC (GCMC) approach that uses a special biased particle insertion/deletion scheme together with dipole and cluster moves and applied it successfully to the restricted primitive model. However, an attempt by us to use the Orkoulas and Panagiotopoulos GCMC approach failed in our study of the aqueous NaCl solution at ambient conditions, because of the presence of the strong hydrogen-bonding network in such solutions.

The most difficult aspect of calculating electrolyte solubility by means of a molecular simulation approach pertains to the solution phase; the modeling of the solid is a separate and less difficult problem. In this work, we developed a hybrid MD−MC approach, called the expanded-ensemble osmotic molecular dynamics (EEOMD) method, that can in principle be used for the molecular-based calculation of solubility. The EEOMD performs simulations at a fixed number of solvent molecules, pressure, temperature and (solid) electrolyte chemical potential. The method combines elements of the constant pressure−constant temperature MD and the expanded-ensemble GCMC approaches. The method does not rely on random insertion/deletion of particles and instead uses the concept of fractional particles. The fractional particles are coupled to the system via a coupling parameter that varies between 0 (no interaction between the fractional particle and the other particles in the system) and 1 (full interaction between the fractional particle and the other particles in the system). The time evolution of the system is governed by the constant pressure−constant temperature equations of motion (MD approach) and is accompanied by random changes in the coupling parameter (MC approach). The coupling-parameter changes are accepted with a probability derived from the expanded-ensemble osmotic partition function corresponding to the prescribed electrolyte chemical potential. The coupling-parameter changes thus mimic the creation/destruction of electrolyte particles: If the coupling parameter becomes 0, the fractional particles disappear from the system, and as the coupling parameter reaches unity, the fractional particles become the full particles.

A random walk in the coupling parameter is facilitated by so-called balancing factors.[11−13] The balancing factors can be viewed to function as a type of bias potential in the umbrella sampling method,[17,18] and they correspond to free-energy differences associated with the coupling-parameter changes. The use of properly optimized values for the balancing factors is critical for implementation of the EEOMD method, because of the large free-energy differences associated with the creation/destruction of ions in the solvent.

The EEOMD method bears similarities to the grand canonical MD approach based on the extended system approach,[19−26] with a hybrid MD−MC grand canonical simulation technique recently proposed by Boinepalli and Attard.[27] In the former methods, the coupling parameter evolves deterministically in time according to a certain equation of motion, whereas in the latter method, the coupling parameter changes stochastically with a transition probability derived from the grand canonical partition function.

As briefly alluded to above, it should be emphasized that the proposed EEOMD simulation method solves only the most computationally demanding part of the problem for prediction of the solubility of solid electrolytes in solvents (i.e., the simulation of electrolyte solutions at fixed total electrolyte chemical potential). The determination of the chemical potential for the pure crystalline electrolyte that would be used as an input to the EEOMD simulations for the solubility prediction is a separate problem.[6] We postpone consideration of this aspect, and of the calculation of electrolyte solubility, to part 2 of this series.

This paper is organized as follows. The derivation and computational background considerations of the EEOMD methodology are presented in section 2. Section 3 defines the molecular models used, and section 4 summarizes the simulation details. Results are presented and discussed in section 5. The final section contains our conclusions.

2. Methodology

We present the derivation and discuss the computational considerations of the EEOMD approach using the case of the

generic 1:1 strong electrolyte solid, AB(s), which dissociates in aqueous solution according to

$$\mathrm{AB(s)} \rightleftharpoons \mathrm{A^+(aq)} + \mathrm{B^-(aq)} \tag{4}$$

This may be used to model a number of systems of interest, including NaCl(s), KF(s), and others. Extension to more complex electrolytes is relatively straightforward.

2.1. Simulation Overview. We consider a system of N_1 water molecules, N_2 (full) ions A^+, and N_3 (full) ions B^-. In addition, the system contains fractional ions of A^+ and B^-, denoted by fA^+ and fB^-, respectively. Because of the global electroneutrality of the system, $N_2 = N_3 \equiv N_{23}$. The fractional ions are coupled to the system via a coupling parameter λ, which controls the interaction between the fractional ion and the other system particles. λ varies between 0 and 1: $\lambda = 0$ corresponds to no interaction between the fractional ion and the other system particles, and $\lambda = 1$ corresponds to full interaction between the fractional ion and the other system particles; λ does not affect the sizes, masses, or velocities of the fractional ions. The EEOMD method combines elements of MD and MC. The system of water molecules and full and fractional A^+ and B^- ions evolves deterministically in time according to the constant pressure−constant temperature equations of motion.[7] After each MD time step, λ is changed randomly, and the λ change is accepted with a probability derived below.

2.2. Coupling-Parameter Changes. To derive the transition probability for the λ change, we start with the expanded-ensemble osmotic partition function[28,29] for the system of N_1 water molecules, N_2 ions A^+, N_3 ions B^-, and two fractional ions fA^+ and fB^-, characterized by λ, at P and T

$$\Omega(N_1, N_2, N_3; P, T) = \sum_{N_2=0}^{\infty}\sum_{N_3=0}^{\infty}\sum_{m=1}^{M}\int_V \exp(N_2\beta\mu_{\mathrm{A^+(aq)}} + N_3\beta\mu_{\mathrm{B^-(aq)}})\exp(\psi_m)\cdot\exp(-\beta PV)\,Q(N_1, N_2, N_3, \lambda_m; V, T)\,\mathrm{d}V \tag{5}$$

In eq 5, V is the system volume, $\beta = 1/(k_B T)$, k_B is Boltzmann's constant, ψ_m are balancing factors of the intermediate λ states m ($\psi_1 \equiv 0$), M is the number of λ states ($m = 1$ corresponds to $\lambda = 0$, and $m = M$ corresponds to $\lambda = 1$), and $Q(N_1, N_2, N_3, \lambda_m; V, T)$ is the canonical partition function.[30] Since we are interested in performing simulations at fixed total AB chemical potential, μ_{AB}, where $\mu_{AB} = \mu_{\mathrm{A^+(aq)}} + \mu_{\mathrm{B^-(aq)}}$, eq 5 becomes

$$\Omega(N_1, N_{23}; P, T) = \sum_{N_{23}=0}^{\infty}\sum_{m=1}^{M}\int_V \exp(N_{23}\beta\mu_{AB})\exp(\psi_m)\cdot\exp(-\beta PV)\,Q(N_1, N_{23}, \lambda_m; V, T)\,\mathrm{dV} \tag{6}$$

The probability of encountering a particular configuration of the system is given by

$$p_m \equiv p(\lambda_m) = \frac{1}{\Omega}\exp(N_{23}\beta\mu_{AB})\exp(\psi_m)\cdot\exp(-\beta PV)\exp[-\beta U(N_1, N_{23}, \lambda_m)] \tag{7}$$

where $U(N_1, N_{23}, \lambda_m) \equiv U_m$ is the system configurational energy of λ state m. The transition probability for a λ change is given as a ratio of the probability (eq 7) of a new λ state n to the probability (eq 7) of a prior λ state o, that is

$$p(\Delta\lambda) = \exp(\psi_n - \psi_o)\exp(-\beta\Delta U_{on}) \tag{8}$$

where $\Delta U_{on} = U_n - U_o$ is the change in U.

The coupling parameter of the new λ state, λ_n, can either be selected from a predefined discrete set of λ values or can vary smoothly on [0, 1] according to the following relation:

$$\lambda_n = \lambda_o + \xi\Delta\lambda_{\max} \tag{9}$$

In eq 9, λ_o is the coupling parameter of the prior λ state, ξ is a random number uniformly distributed in [−1, 1], and $\Delta\lambda_{\max}$ is the maximum allowable change in λ. In the case of smoothly varying λ, a value of ψ corresponding to λ_n is obtained by interpolation on a discrete set of ψ values. In this work, we used the smoothly varying λ approach, since it allowed us to use a larger MD time step.

The balancing factors are, in principle, arbitrary. However, to facilitate transitions between particular λ states, as well as to guarantee that all λ states are visited uniformly, $\psi_n - \psi_o$ should be proportional to the excess chemical potential associated with the transition of the system from λ_o to λ_n, that is

$$\psi_n - \psi_o = \beta\Delta\mu^{\mathrm{ex}}_{AB}(\lambda_o \rightarrow \lambda_n) \equiv \beta[\mu^{\mathrm{ex}}_{AB}(N_1, N_{23}, \lambda_n) - \mu^{\mathrm{ex}}_{AB}(N_1, N_{23}, \lambda_o)] \tag{10}$$

Equation 10 suggests that a convenient choice for ψ_m is

$$\begin{aligned}\psi_m &= \beta\mu^{\mathrm{ex}}_{AB}(N_1, N_{23}, \lambda_m)\\ &= \omega_m\beta\mu^{\mathrm{ex}}_{AB}(N_1, N_{23})\\ &= \omega_m\left[\beta\mu_{AB} - 2\ln\left(\frac{N_{23}+1-\delta_{1,m}}{\beta P^0 V}\right) - \beta\mu^0_{\mathrm{A^+}} - \beta\mu^0_{\mathrm{B^-}}\right]\end{aligned} \tag{11}$$

where we have introduced normalized balancing factors $\omega_m = \psi_m/\psi_M$; $\omega_1 \equiv 0$ and $\omega_M \equiv 1$. In eq 11, $\delta_{1,m}$ is Kronecker's delta, P^0 is the standard-state pressure, taken to be 1 bar, and $\mu^0_{\mathrm{A^+}}$ and $\mu^0_{\mathrm{B^-}}$ are, respectively, the standard chemical potentials of the A^+ and B^- ions in the ideal-gas (IG) state at T and P^0. By inserting eq 11 into eq 8, we obtain the final expression for the transition probability for a λ change

$$p(\Delta\lambda) = \exp\left\{(\omega_n - \omega_o)\left[\beta\mu_{AB} - 2\ln\left(\frac{N_{23}+1-\delta_{1,n}}{\beta P^0 V}\right) - \beta\mu^0_{\mathrm{A^+}} - \beta\mu^0_{\mathrm{B^-}}\right]\right\}\cdot\exp(-\beta\Delta U_{on}) \tag{12}$$

Note that if the prior and new λ states become end λ states, eq 12 gives the usual transition probability for insertion/deletion of (full) A^+ and B^- ions. Also note that, if $\omega = \lambda$, eq 12 reduces to $p(\Delta\lambda)$, analogous to that in the Boinepalli and Attard GCMD approach.[27]

When the fractional ions reach an end λ state, we proceed as follows: If λ becomes 0, we decide randomly whether the fractional ions are removed from the system and randomly selected full A^+ and B^- ions become new fractional ions with $\lambda = 1$, or whether an increase in λ for the existing fractional ions is performed. Similarly, if λ reaches 1, we decide randomly whether the fractional ions become full A^+ and B^- ions and new fractional ions with $\lambda = 0$ are randomly inserted into the system, or whether a decrease in λ for the existing fractional ions is performed. Since the new fractional ions have $\lambda = 0$, their insertions pose no problem in the calculation. The velocities of the new fractional ions are assigned from the Maxwell−Boltzmann distribution corresponding to T. This procedure guarantees that the end λ states are indistinguishable from each other.

2.3. Chemical Potential of Ionic Species in Solution. To test the EEOMD method, we devised an approach to independently determine the total AB chemical potential, μ_{AB}, in water, given by the sum of the chemical potentials of the individual A^+ and B^- ions, which can be split into their IG and excess (ex) parts

$$\begin{aligned}\beta\mu_{AB} &= \beta\mu_{A^+(aq)} + \beta\mu_{B^-(aq)} \\ &= \beta(\mu^{IG}_{A^+} + \mu^{IG}_{B^-}) + \beta(\mu^{ex}_{A^+} + \mu^{ex}_{B^-}) \\ &= \beta(\mu^0_{A^+} + \mu^0_{B^-}) + 2\ln\left(\frac{N_{23}}{\beta P^0\langle V\rangle}\right) + \beta\mu^{ex}_{AB} \end{aligned} \quad (13)$$

where $\beta(\mu^0_{A^+} + \mu^0_{B^-}) + 2\ln[N_{23}/(\beta P^0\langle V\rangle)] \equiv \beta\mu^{IG}_{AB}$, $\beta\mu^{ex}_{AB} \equiv \beta(\mu^{ex}_{A^+} + \mu^{ex}_{B^-})$, and $\langle . \rangle$ denotes an ensemble average. We evaluated $\beta\mu^{ex}_{AB}$ by the thermodynamic integration technique[6] as

$$\beta\mu^{ex}_{AB} = \beta\int_0^1 \left\langle \frac{\partial U(N_1, N_{23}, \lambda)}{\partial\lambda}\right\rangle d\lambda \quad (14)$$

and by the expanded-ensemble method[11−13] as

$$\beta\mu^{ex}_{AB} = \psi(\lambda = 1) - \psi(\lambda = 0) + \ln\left[\frac{p(\lambda = 0)}{p(\lambda = 1)}\right] \quad (15)$$

where $p(\lambda = 0)$ and $p(\lambda = 1)$ are probabilities of visiting the end λ states.

The thermodynamic integration technique relies on a series of constant pressure-constant temperature simulations for systems of N_1 water molecules, N_2 ions A^+, N_3 ions B^-, and two fractional ions, fA^+ and fB^- with different λ values; the results of these simulations are values of $\langle\partial U/\partial\lambda\rangle$ for particular λ's. Then, the $\langle\partial U/\partial\lambda\rangle$ values are fitted to a convenient functional form in λ, and the functional form is integrated analytically between 0 and 1 to obtain the value of $\beta\mu^{ex}_{AB}$. The expanded-ensemble method evaluates $\beta\mu^{ex}_{AB}$ in a single simulation run that combines constant pressure−constant temperature MD for the system of N_1 water molecules, N_2 ions A^+, N_3 ions B^-, and two fractional ions, fA^+ and fB^-, with an MC walk in λ. The λ changes are accepted with probability[11−13]

$$p(\Delta\lambda) = \frac{\exp(\psi_n)\exp[-\beta U(N_1, N_{23}, \lambda_n)]}{\exp(\psi_o)\exp[-\beta U(N_1, N_{23}, \lambda_o)]} \quad (16)$$

2.4. Balancing Factors. The use of the expanded-ensemble method requires prior determination of the balancing factors, ψ_m, which must be chosen so that the probabilities of visiting particular λ states, p_m, do not become too small. Wilding and Müller[31] proposed an iterative procedure for the estimation of ψ_m, which allows the system to visit each λ state with p_m values of similar magnitude. This procedure requires several trial runs; its implementation becomes rather tedious and requires certain expertise. Recently, Åberg et al.[32] developed an adaptive expanded-ensemble method that uses probability density estimation to continuously optimize ψ_m.

Since we use the thermodynamic integration technique for determination of μ_{AB}, we may obtain ψ_m as a byproduct of the integration as follows. As already mentioned, the difference in ψ_m between two neighboring λ states i and j should be proportional to the excess chemical potential associated with the transition of the system from λ_i to λ_j, $\beta\Delta\mu^{ex}_{AB}(\lambda_i \rightarrow \lambda_j)$ (see eq 10). $\beta\Delta\mu^{ex}_{AB}(\lambda_i \rightarrow \lambda_j)$ can be expressed within the framework of the thermodynamic integration technique (see eq 14) as

$$\beta\Delta\mu^{ex}_{AB}(\lambda_i \rightarrow \lambda_j) = \beta\int_{\lambda_i}^{\lambda_j}\left\langle\frac{\partial U(\lambda)}{\partial\lambda}\right\rangle d\lambda \quad (17)$$

as well as within the framework of the expanded-ensemble method (see eq 15) as

$$\beta\Delta\mu^{ex}_{AB}(\lambda_i \rightarrow \lambda_j) = \psi(\lambda_j) - \psi(\lambda_i) + \ln\left[\frac{p(\lambda_i)}{p(\lambda_j)}\right] \quad (18)$$

ψ_m, in addition to facilitating transitions between neighboring λ states, should also guarantee that all λ states are visited with a similar frequency, that is

$$\frac{p(\lambda_i)}{p(\lambda_j)} \approx 1 \quad (19)$$

By comparing eqs 17 and 18, and by using condition 19, we obtain a working equation for the estimation of the balancing factors

$$\psi(\lambda_j) - \psi(\lambda_i) \approx \beta\int_{\lambda_i}^{\lambda_j}\left\langle\frac{\partial U(\lambda)}{\partial\lambda}\right\rangle d\lambda,\ \psi(\lambda = 0) \equiv 0 \quad (20)$$

In practice, it is not usually necessary to determine ψ_m for each particular system composition (N_1, N_{23}) which is sampled during an EEOMD simulation. If the free-energy surface does not change significantly relative to k_BT for differing values of (N_1, N_{23}), then it is sufficient to determine ψ_m only at a single composition (e.g., at infinite dilution). We also found that it is useful to further optimize the values of ψ_m, as obtained from eq 20, to improve the uniformity of the p_m distribution. We performed this additional optimization according to the Wilding and Müller iterative updating scheme,[31] using

$$\psi^{(k)}_m = \psi^{(k-1)}_m - \ln\left[\frac{p(\lambda_m)}{p(\lambda_1)}\right]^{(k-1)} \quad (21)$$

3. Molecular Model

To implement our procedure, we must choose a particular electrolyte, AB(s). Here, we test our algorithm by choosing molecular parameters for a model of an aqueous solution of the ions Na^+ and Cl^-, corresponding to the strong electrolyte NaCl(s).

We model water by the SPC/E model[33] and sodium and chloride ions as charged Lennard-Jones (LJ) particles.[34] The intermolecular potential energy between water atoms, ions, and water atoms−ions is calculated as a sum of LJ and Coulombic interactions

$$u_{ab} = 4\epsilon_{ab}\left[\left(\frac{\sigma_{ab}}{r_{ab}}\right)^{12} - \left(\frac{\sigma_{ab}}{r_{ab}}\right)^{6}\right] + \frac{q_a q_b e^2}{4\pi\epsilon_0 r_{ab}} \quad (22)$$

where r_{ab} is the distance between sites a and b in two different particles, ϵ_{ab} and σ_{ab} are the LJ cross parameters for sites a and b in these particles, q_a and q_b are the partial charges on these sites, ϵ_0 is the permittivity of vacuum, and e is the elementary charge. The LJ parameters ϵ_{ab} and σ_{ab} are expressed using the Lorentz−Berthelot mixing rules[7] as

$$\epsilon_{ab} = \sqrt{\epsilon_a\epsilon_b} \quad \sigma_{ab} = \frac{\sigma_a + \sigma_b}{2} \quad (23)$$

TABLE 1: The Lennard-Jones Well Depth ϵ_l and Size σ_l, Partial Charges q_l for Water Atoms and Sodium, and Chloride Ions, Together with the Water Geometry; k_B Is Boltzmann's Constant

		SPC/E H_2O[33]		
atom	ϵ/k_B (K)	σ (Å)	q (e)	geometry
O	78.2	3.166	−0.8476	O−H: 1.00 Å
H	0	0	+0.4238	H−O−H: 109.47°
		Ions[34]		
ion	ϵ/k_B (K)	σ (Å)	q (e)	
Na^+	65.42	2.35	+1.0	
Cl^-	50.32	4.40	−1.0	

where ϵ_l and σ_l are the LJ well depth and size of a site l; l = a, b. The values of the potential parameters together with the water geometry are given in Table 1. We used potential parameters for the sodium and chloride ions determined by Smith and Dang[34] by fitting the ϵ and σ values of the ions to gas-phase binding enthalpy data for small sodium and chloride ion−water clusters using the SPC/E water model. The molecular model used has been found to be adequate for simulations of the structure and thermodynamics of aqueous NaCl solutions at ambient conditions[35] as well as at high pressures and temperatures.[36]

The fractional sodium and chloride ions, fNa^+ and fCl^-, were coupled to the system by scaling the LJ cross-energy parameters and the charges. We used two methods for the fractional-ion coupling, to test for the existence of simulation instabilities in the vicinity of $\lambda = 0$.[37] A linear coupling (denoted by LC)

$$\epsilon_{fNa^+,b} = \lambda\epsilon_{Na^+,b}\ \epsilon_{fCl^-,b} = \lambda\epsilon_{Cl^-,b} \quad (b = O, H, Na^+, Cl^-)$$

$$q_{fNa^+} = \lambda q_{Na^+}\ q_{fCl^-} = \lambda q_{Cl^-} \tag{24}$$

and two different nonlinear couplings (denoted by NLC1 and NLC2, respectively)

$$\epsilon_{fNa^+,b} = \lambda^5\epsilon_{Na^+,b}\ \epsilon_{fCl^-,b} = \lambda^5\epsilon_{Cl^-,b} \quad (b = O, H, Na^+, Cl^-)$$

$$q_{fNa^+} = \lambda^{2.5} q_{Na^+}\ q_{fCl^-} = \lambda^{2.5} q_{Cl^-} \tag{25}$$

$$\epsilon_{fNa^+,b} = \lambda^5\epsilon_{Na^+,b}\ \epsilon_{fCl^-,b} = \lambda^5\epsilon_{Cl^-,b} \quad (b = O, H, Na^+, Cl^-)$$

$$q_{fNa^+} = \lambda^3 q_{Na^+}\ q_{fCl^-} = \lambda^3 q_{Cl^-} \tag{26}$$

4. Simulation Details

We used a cubic simulation box containing 256 particles, with periodic boundary conditions applied to the center-of-mass (COM) separations. The COM cutoff radius was equal to the half-box length. The LJ long-range corrections for the configurational energy and the pressure were included, assuming that the radial distribution functions are unity beyond the COM cutoff radius. The equations of translational and rotational motion were solved by the Gear predictor−corrector algorithm of the fifth and fourth orders,[7] respectively, with an integration step between 1.5 and 2.5 fs. The pressure and temperature were kept constant by applying the Andersen barostat[38] and the Berendsen thermostat,[39] respectively. The membrane mass M in the Andersen barostat and the coupling time constant τ_T in the Berendsen thermostat were set to $5\cdot10^{-4}\ m_O/\sigma_O^4$ and 0.01 ps, respectively, where m_O is the mass of oxygen atoms. We used the Berendsen thermostat, since it is robust and is well-suited for combined MD/MC studies of open systems.[40] Use of the Berendsen thermostat has, however, the general disadvantage that fluctuations of global properties cannot be used to obtain thermodynamic properties.[39] The λ changes were performed after each MD time step with $\Delta\lambda_{max} = 0.1$. The Coulombic long-range interactions were incorporated by means of an Ewald sum,[7] with separation parameter α equal to $6/L$, where L is the box length. The maximum magnitude of the dimensionless k vector was $k_{max} = 6.16$.

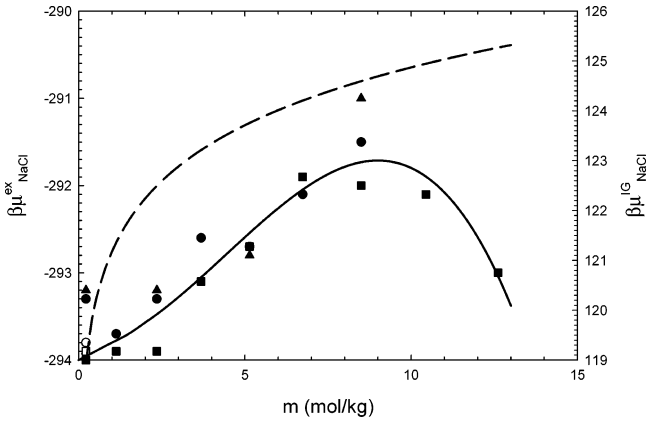

Figure 1. Excess and ideal-gas chemical potentials for sodium chloride in water, $\beta\mu^{ex}_{NaCl}$ and $\beta\mu^{IG}_{NaCl}$, respectively, as a function of salt concentration, expressed in terms of molality, m, at a temperature of 300 K and a pressure of 1 bar. ○, $\beta\mu^{ex}_{NaCl}$ from thermodynamic integration technique with LC; △, $\beta\mu^{ex}_{NaCl}$ from thermodynamic integration technique with NLC1; ●, $\beta\mu^{ex}_{NaCl}$ from thermodynamic integration technique with NLC2; ▲, $\beta\mu^{ex}_{NaCl}$ from two-step thermodynamic integration technique with NLC2; □, $\beta\mu^{ex}_{NaCl}$ from expanded-ensemble method with LC; ■, $\beta\mu^{ex}_{NaCl}$ from expanded-ensemble method with NLC1. Error bars corresponding to relative error in $\beta\mu^{ex}_{NaCl}$ equal to ∼1% and ∼0.5% in the case of the thermodynamic integration technique and in the case of the expanded-ensemble method, respectively, are not drawn since they would be beyond the scale of the graph. The solid line represents regression fits of the $\beta\mu^{ex}_{NaCl}$ simulation results using the simulation uncertainties as weights. The dashed line denotes $\beta\mu^{IG}_{NaCl}$.

5. Results and Discussion

We performed all simulations for a model corresponding to an aqueous sodium chloride solution at $T = 300$ K and $P = 1$ bar, and at salt concentrations up to a molality m of 13 mol/kg. (The experimental solubility of NaCl in water corresponds to $m = 6.160$ mol/kg.[41])

5.1. Chemical Potential of NaCl in Ambient Water and Balancing Factors. *A. Thermodynamic Integration Technique.* We applied the thermodynamic integration methodology to calculate the excess chemical potential of NaCl in water, $\beta\mu^{ex}_{NaCl}$, according to eq 14, and the results are plotted, together with the IG chemical potential $\beta\mu^{IG}_{NaCl}$, in Figure 1, as a function of the salt concentration. Intermediate λ points were chosen uniformly with step-size 0.1 in the interval between 0.1 and 1.0, and more frequently close to zero, because of the repulsive character of the interaction in the vicinity of $\lambda = 0$; the lengths of the simulation runs were 2.5 ns. In the case of LC, we observed that the integrand of eq 14 sharply increased to infinity as $\lambda \to 0$. However, this increase was not accompanied by simulation instabilities that are caused by unrealistic intermolecular attractions appearing at certain configurations sampled during the simulations. We thus used the Widom test-particle-insertion method to evaluate the corresponding contributions to $\beta\mu^{ex}_{NaCl}$ at these small λ values. This was possible, because the fractional ions at small λ values are

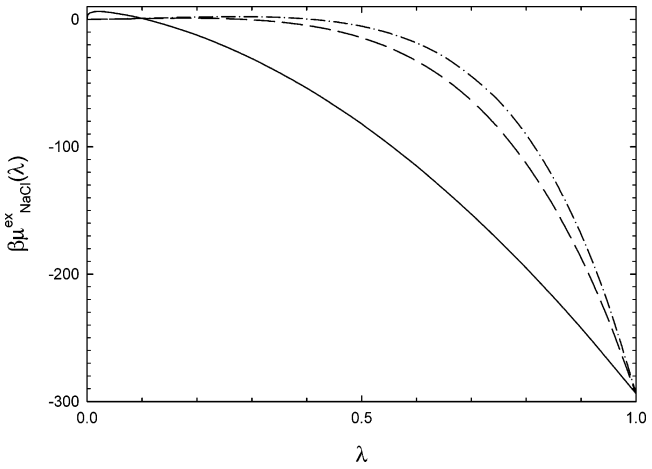

Figure 2. Excess chemical potential of sodium chloride in water, $\beta\mu^{ex}_{NaCl}$ (λ), as a function of the coupling parameter, λ, from simulations using the thermodynamic integration technique at a temperature of 300 K and a pressure of 1 bar, and at infinite dilution. The solid line corresponds to linear coupling, and the dashed and dash−dotted lines correspond to NLC1 and NLC2, respectively.

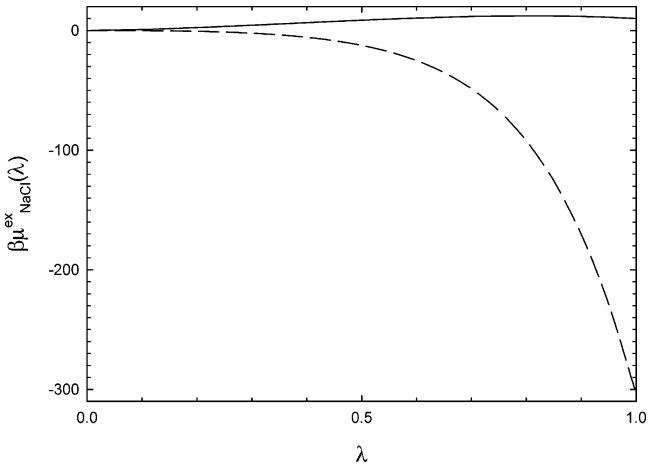

Figure 3. Contributions to the excess chemical potential of sodium chloride in water, $\beta\mu^{ex}_{NaCl}(\lambda)$, from the Lennard-Jones (solid line) and the Coulombic (dashed line) parts of the interactions as a function of the coupling parameter, λ, from simulations with the two-step thermodynamic integration technique associated with NLC2 at a temperature of 300 K and a pressure of 1 bar, and at infinite dilution.

only weakly coupled to the system. In the cases of NLC1 and NLC2, the integrand of eq 14 smoothly approached zero as $\lambda \rightarrow 0$.

Figure 2 shows the variation of the NaCl excess chemical potential, $\beta\mu^{ex}_{NaCl}(\lambda)$, as a function of λ, for the different couplings at "infinite" dilution (i.e., for a system of 254 water molecules and 2 fractional ions Na^+ and Cl^-). We see that all couplings yield the same values of $\beta\mu^{ex}_{NaCl} \equiv \beta\mu^{ex}_{NaCl}(\lambda = 1)$ within the accuracy of the thermodynamic integration method. We estimate that the relative errors in $\beta\mu^{ex}_{NaCl}$ are ~1%. Further, the $\beta\mu^{ex}_{NaCl}(\lambda)$ values for all couplings exhibit similar behavior. First, there occurs a growth of $\beta\mu^{ex}_{NaCl}(\lambda)$ with λ corresponding to the positive free-energy change for creating a cavity in the water system (the effects of the repulsive part of the water−ion interaction); then, the attractive (energetic) part of the water−ion interaction plays a more important role, and $\beta\mu^{ex}_{NaCl}(\lambda)$ ultimately decreases with increasing λ. The growth of $\beta\mu^{ex}_{NaCl}(\lambda)$ is very rapid in the case of LC and is very slow in the cases of NLC1 and NLC2. On the other hand, the decrease of $\beta\mu^{ex}_{NaCl}(\lambda)$ with increasing λ is nearly linear in the case of LC and is rather steep in the cases of NLC1 and NLC2. The steepness of the decrease increases with the exponent on λ in scaling the charges on the fractional ions (1, 2.5, and 3 for the LC, NLC1, and NLC2, respectively; see eqs 24, 25, and 26]. From the point of view of the EEOMD method, it would be desirable that $\beta\mu^{ex}_{NaCl}(\lambda)$ vary linearly with λ. Hence, we attempted to reduce the exponent on λ for the nonlinear couplings below the value of 2.5. However, it resulted in simulation instabilities at small λ values.

To understand the separate roles of the LJ and the Coulombic parts of the interactions on $\beta\mu^{ex}_{NaCl}(\lambda)$, we also carried out a two-step thermodynamic integration procedure to calculate $\beta\mu^{ex}_{NaCl}$. First, we performed the integration with the charges on the fractional ions Na^+ and Cl^- switched off and evaluated the contribution to $\beta\mu^{ex}_{NaCl}(\lambda)$ from the LJ part of the interaction. Then, starting from the fractional ions Na^+ and Cl^- with full LJ interactions turned on, we carried out the integration with respect to the charges on the fractional ions Na^+ and Cl^-, to calculate the contribution to $\beta\mu^{ex}_{NaCl}(\lambda)$ from the Coulombic part of the interaction. The results of this two-step thermodynamic integration approach with NLC2 of the ions at infinite dilution are shown in Figure 3. We see that the Coulombic contribution to $\beta\mu^{ex}_{NaCl}(\lambda)$ dominates over the LJ contribution and that the Coulombic contribution to $\beta\mu^{ex}_{NaCl}(\lambda)$ alone almost matches the corresponding total $\beta\mu^{ex}_{NaCl}(\lambda)$ from Figure 2. The numerical value of $\beta\mu^{ex}_{NaCl}$ from the two-step thermodynamic integration approach corresponds to the sum of the LJ and Coulombic contributions to $\beta\mu^{ex}_{NaCl}(\lambda)$ at $\lambda = 1$, and this value agrees within the accuracy of the method with the results from Figure 2.

TABLE 2: Values of the Balancing Factors ψ at Intermediate λ Points for the Linear Coupling (LC), eq 24, and Nonlinear Coupling Number 1 (NLC1), eq 25

LC		NLC1	
λ	ψ	λ	ψ
0.0	0.00	0.00	0.00
$2.0\cdot10^{-5}$	0.05	0.10	0.10
$1.0\cdot10^{-4}$	0.25	0.20	0.70
$2.0\cdot10^{-4}$	0.65	0.25	1.35
$5.0\cdot10^{-4}$	1.35	0.30	1.70
$1.0\cdot10^{-3}$	2.00	0.35	1.65
$2.0\cdot10^{-3}$	2.75	0.40	0.80
$5.0\cdot10^{-3}$	3.95	0.45	−1.15
0.01	5.00	0.50	−4.65
0.03	6.70	0.55	−10.20
0.10	6.30	0.60	−18.45
0.20	−1.50	0.65	−30.20
0.30	−15.90	0.70	−46.35
0.40	−36.75	0.75	−67.70
0.50	−64.20	0.80	−95.40
0.60	−98.05	0.85	−130.55
0.70	−138.10	0.90	−174.60
0.80	−184.35	0.95	−229.00
0.90	−236.85	1.00	−294.00
1.00	−293.95		

Finally, the results of the thermodynamic integration technique were used to determine the values of the balancing factor ψ_m according to eq 20 for LC and NLC1 at infinite dilution. In addition, these values of ψ_m were further optimized according to eq 21 to improve the uniformity of the distribution over the λ values. The final values of ψ_m are summarized in Table 2.

B. Expanded-Ensemble Method. We applied the expanded-ensemble methodology with ψ_m optimized at infinite dilution for the calculation of the excess chemical potential of NaCl in

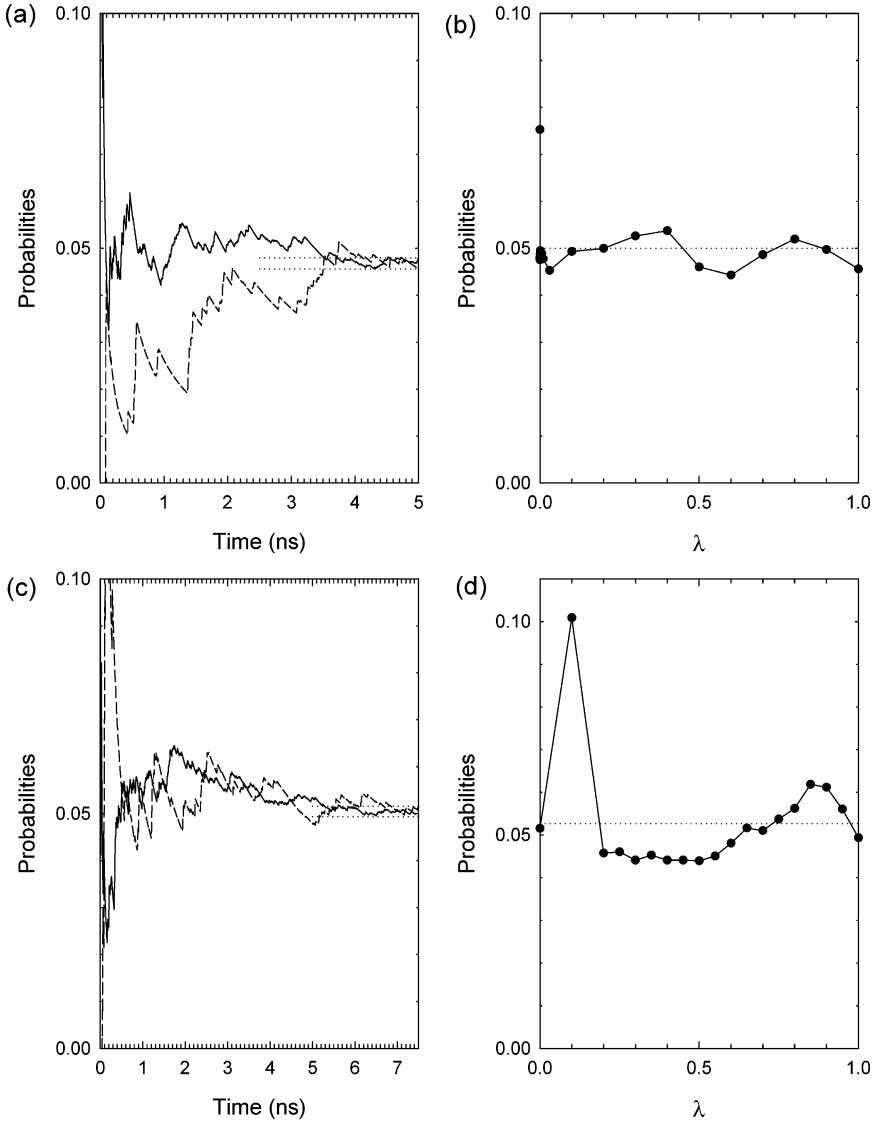

Figure 4. (a, c) Convergence profiles for probabilities at the end λ-states, $p(\lambda = 0)$ (solid lines) and $p(\lambda = 1)$ (dashed lines), and (b, d) distributions of the probabilities over intermediate λ-states for LC (a, b) and for NLC1 (c, d) obtained by simulations with the expanded-ensemble method at a temperature of 300 K and a pressure of 1 bar, and at infinite dilution.

water, $\beta\mu^{\text{ex}}_{\text{NaCl}}$, according to eq 15. The intermediate λ points were chosen in a similar way to the case of the thermodynamic integration technique. The lengths of the simulation runs were between 5 ns and 7.5 ns, with λ changes after each MD time step. The results for $\beta\mu^{\text{ex}}_{\text{NaCl}}$ obtained by the expanded-ensemble method are plotted in Figure 1 as a function of the salt concentration (squares).

Figure 4 shows convergence profiles for the probabilities at the end λ states, $p(\lambda = 0)$ and $p(\lambda = 1)$, and the distributions of the probabilities p_m over intermediate λ states for LC and NLC1 at infinite dilution. Figure 4 confirms, as expected, that the p_m distribution is roughly uniform (except for a λ value in the vicinity of zero), because of the optimization of ψ_m at infinite dilution.

In Figure 5, we show additional convergence profiles for the probabilities $p(\lambda = 0)$ and $p(\lambda = 1)$ and the p_m distributions for NLC1 at finite salt concentrations. We see that the p_m distributions remain quite uniform at these concentrations. This suggests that the free-energy surface for the ambient aqueous NaCl solution does not change significantly relative to k_BT for the simulated salt concentrations and that the ψ_m values determined at infinite dilution are well-suited for the EEOMD simulations.

It is evident from Figures 4 and 5, and from comparison of the values of ψ_m and $\beta\mu^{\text{ex}}_{\text{NaCl}}$, that the main contribution to $\beta\mu^{\text{ex}}_{\text{NaCl}}$ arises from the fixed difference $\psi_M - \psi_1$; see eq 15. The term $\ln(p_1/p_M)$ obtained from the simulations is thus only a small correction to this difference, and we estimated the relative statistical error to be small, up to 0.5% (smaller than in the case of the thermodynamic integration technique).

Finally, the results for $\beta\mu^{\text{ex}}_{\text{NaCl}}$ obtained from the thermodynamic integration technique and from the expanded-ensemble method were used to evaluate the (full) chemical potential of NaCl in water, $\beta\mu_{\text{NaCl}}$, according to eq 13. The values for $\mu^0_{\text{Na}^+}$ and $\mu^0_{\text{Cl}^-}$ were taken from tabular compilations of thermochemical data,[42] and the results for $\beta\mu_{\text{NaCl}}$ are plotted in Figure 6 as a function of the salt concentration. We see that $\beta\mu_{\text{NaCl}}$ goes through a minimum at $m \approx 9.5$ mol/kg.

5.2. Aquesous NaCl Solution Simulations at Fixed Chemical Potential. We carried out a series of EEOMD simulations for an ambient aqueous NaCl solution at different values of the total NaCl chemical potential: $\{(N_1, \beta\mu_{\text{NaCl}})\} = \{(246, -173.0), (236, -171.5), (226, -170.0), (216, -169.0), (206, -167.5)\}$, and we measured the number of Na^+ and Cl^- ions resulting

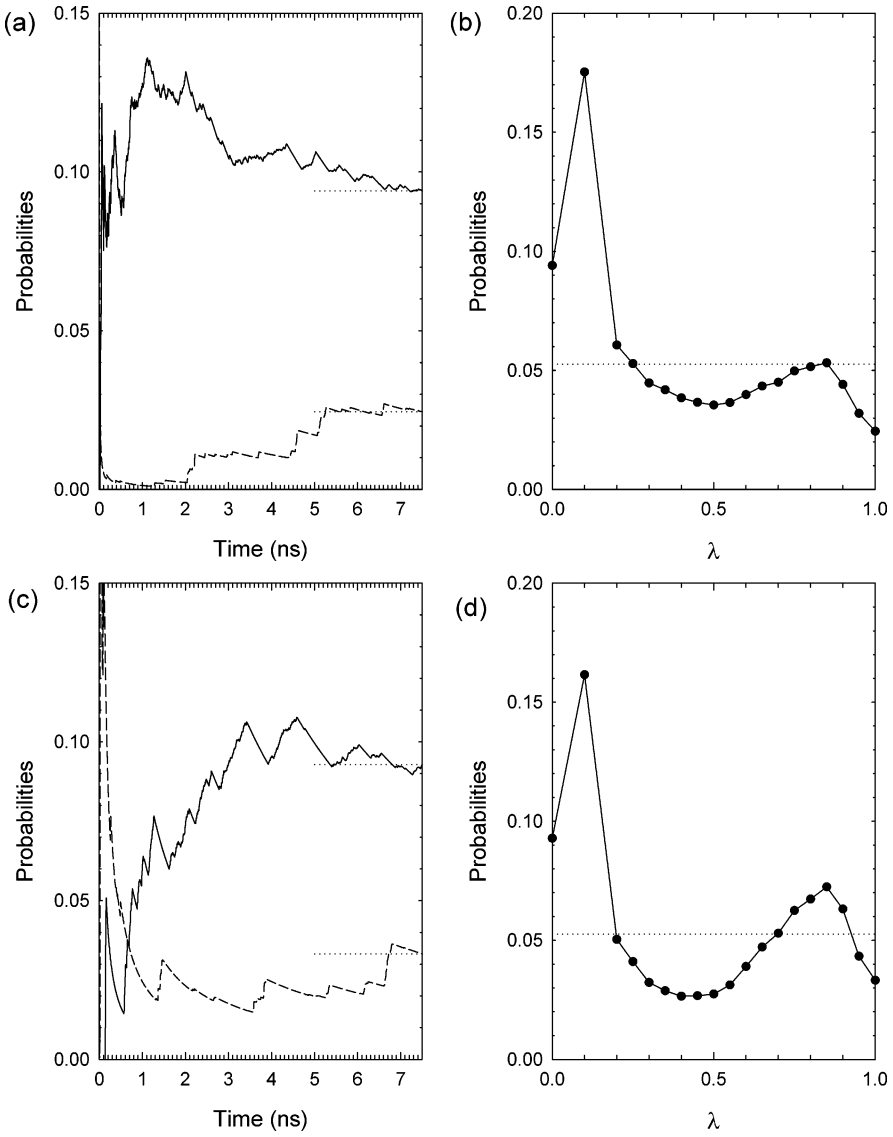

Figure 5. (a, c) Convergence profiles for the probabilities at the end λ-states, $p(\lambda = 0)$ (solid lines) and $p(\lambda = 1)$ (dashed lines), and (b, d) distributions of the probabilities over intermediate λ states obtained by simulations with the expanded-ensemble method for NLC1 at a temperature of 300 K and a pressure of 1 bar, and at concentrations $m = 5.140$ kg/mol (a, b) and $m = 12.616$ kg/mol (c, d).

from the simulations. We used ψ_m values optimized at infinite dilution corresponding to the LC and NLC1 of eqs 24 and 25, respectively. In contrast to discrete λ changes, used in the calculation of $\beta\mu^{ex}_{NaCl}$ by the expanded-ensemble method, the EEOMD method performs a random walk in λ according to eq 9. The values of ψ_m were thus fitted to cubic splines, and the ψ values for the different λ values, which were sampled during the simulations, were obtained by interpolation using these splines. The lengths of the EEOMD simulation runs were between 20 ns (low salt concentrations) and 28 ns (high salt concentrations); the convergence of each simulations was monitored using running profiles for the number of Na^+ and Cl^- ions.[43]

The EEOMD simulation of the ambient aqueous NaCl solution at $(N_1, \beta\mu_{NaCl}) = (206, -167.5)$ did not converge, that is, the running profile of the number of ions did not shown oscillation around an equilibrium value but, rather, exhibited detached time periods where the number of ions oscillated around metastable values. Hence, instead of fixing P, we fixed V to a value corresponding to $\langle V \rangle$ obtained from a previous measurement of the chemical potential; the resulting simulation converged. Interestingly, the aqueous NaCl solution at $\beta\mu_{NaCl} = -167.5$ is above the experimental solubility limit, whereas the aqueous NaCl solutions at $\{\beta\mu_{NaCl}\} = \{-173.0, -171.5, -170.0, -169.0\}$ lie in the experimental one-phase region.[41] The convergence problem at fixed P may be evidence that the system is in the two-phase region. It should be mentioned that it is not surprising that EEOMD simulations at fixed V converge in the two-phase region, while EEOMD simulations at fixed P do not converge. It is well-known that constant V simulations can be used in two-phase regions to determine, for example, van der Waals-like loops in pressure[44] or in chemical potential,[45] while constant P simulations in two-phase regions either do not converge or exhibit hysteresis effects.[7]

We did not observe any differences in efficiency between the two coupling methods used, and the results from EEOMD with LC agreed with those from EEOMD with NLC1. The results of the EEOMD simulations for the ambient aqueous NaCl solutions are plotted in Figure 7, and they are summarized in Table 3. The reported values in Table 3 represent averages of the simulation results from the EEOMD with LC and from the EEOMD with NLC1.

The EEOMD simulation results in Figure 7 are plotted as $\beta\mu_{NaCl}$ versus molality m together with results from the chemical

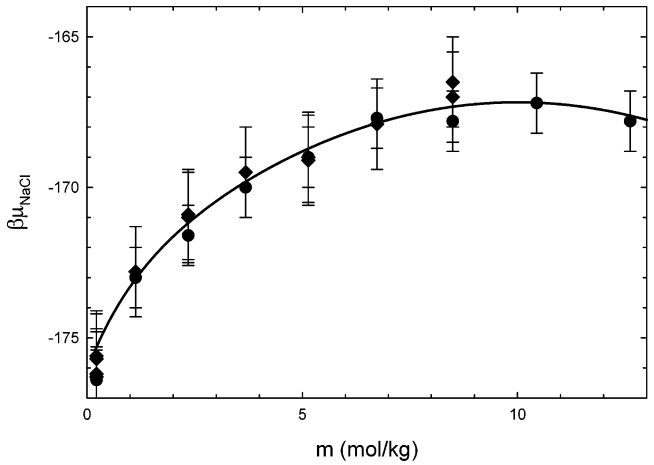

Figure 6. Chemical potential of sodium chloride in water, $\beta\mu_{NaCl}$, as a function of salt concentration expressed in terms of molality, m, at a temperature of 300 K and a pressure of 1 bar. Filled circles denote the simulation results from the thermodynamic integration technique, and filled diamonds correspond to simulation results from the expanded-ensemble method. The solid line represents regression fits of the $\beta\mu_{NaCl}$ simulation values using the simulation uncertainties as weights.

TABLE 3: Simulation Results for Open Aqueous NaCl Solutions at a Temperature of 300 K and a Pressure of 1 Bar, as Obtained from the EEOMD Simulations[a]

$\beta\mu_{NaCl}$	N_1	u^{ex} (kJ/mol)	ρ (kg/m^3)	N_{23}	m (kg/mol)
−173.0	246	−54.68(130)	1037(15)	4.51(42)	1.02(10)
−171.5	236	−67.25(216)	1072(16)	8.58(53)	2.02(12)
−170.0	226	−85.32(269)	1116(17)	14.30(63)	3.51(15)
−169.0	216	−104.82(327)	1161(18)	20.35(72)	5.23(18)
−167.5[b]	206	−126.50(271)	1219(19)	26.88(37)	7.24(10)

[a] $\beta\mu_{NaCl}$ is the prescribed chemical potential of NaCl, N_1 is the prescribed number of water molecules, u^{ex} is the excess internal energy, ρ is the density, N_{23} is the number of Na^+ or Cl^- ions, and m is the molality. The simulation uncertainties are given in the parentheses. [b] Simulation at fixed volume.

potential measurement (Figure 7a) and as the density of the NaCl solution ρ as a function of m (Figure 7b). Figure 7a exhibits perfect consistency of the results from the EEOMD simulations and the chemical potential measurement simulations. In Figure 7b, we see excellent agreement between our EEOMD results and the constant pressure−constant temperature MD results of Brodholt.[36] Both simulation results for ρ also agree very well with the corresponding experimental data.[46,47]

6. Conclusions

We developed a simulation tool, the expanded-ensemble osmotic molecular dynamics (EEOMD) method, to study open (at fixed total chemical potential) electrolyte solution systems. The EEOMD approach performs simulations at a fixed number of solvent molecules, pressure, temperature, and overall electrolyte chemical potential. The EEOMD approach combines elements of the constant pressure−constant temperature molecular dynamics and the expanded-ensemble grand canonical Monte Carlo and uses the concept of fractional particles. The time evolution of the system is governed by the constant pressure−constant temperature equations of motion and is accompanied by random changes in the coupling parameter that characterizes the fractional particles. The EEOMD method, in contrast to Monte Carlo methods for open systems, can take full advantage of parallelism, since it relies on the molecular dynamics approach. It is well-known that molecular dynamics

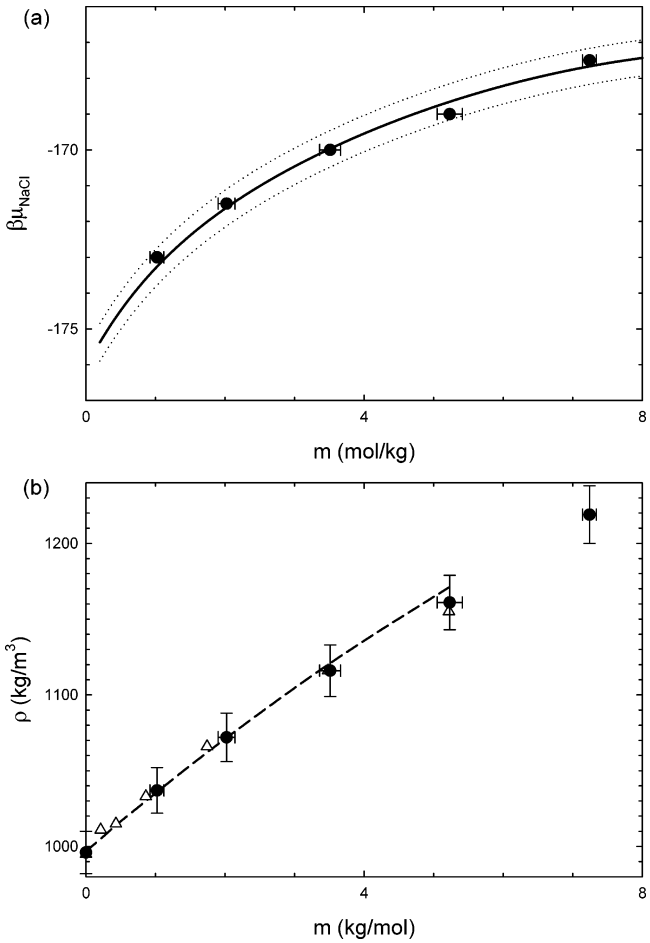

Figure 7. Simulation results for open aqueous NaCl solutions obtained from the EEOMD method at a temperature of 300 K and a pressure of 1 bar. (a) Results for the chemical potential of sodium chloride in water $\beta\mu_{NaCl}$ vs molality m. (b) Density of the NaCl solution, ρ, as a function of m. Filled circles represent the EEOMD simulation results, and open triangles are the constant pressure−constant temperature results of Brodholt[36] for ρ. The solid line represents regression fits of the $\beta\mu_{NaCl}$ simulation values using the simulation uncertainties as weights, and the dotted lines denote the error margin of the $\beta\mu_{NaCl}$ simulation values. The dashed line represents the experimental data for ρ.[46,47]

approaches, in contrast to Monte Carlo approaches, can be relatively easily and straightforwardly parallelized.

The EEOMD methodology was derived using the case of a generic 1:1 strong electrolyte and was tested using a molecular model of NaCl dissolved in water at ambient conditions. The EEOMD simulations of open aqueous NaCl solutions showed an excellent agreement with our independent calculations of NaCl chemical potentials in water, performed by the thermodynamic integration technique and by the expanded-ensemble method, and with the constant pressure−constant temperature molecular dynamics simulations of Brodholt.[36]

By performing simulations for which the electrolyte chemical potential is set equal to the solid electrolyte chemical potential, the EEOMD method in principle allows the direct simulation of electrolyte solubilities. This requires an independent method to calculate the solid electrolyte's chemical potential at given pressure and temperature. This will be considered in a subsequent paper and combined with the EEOMD method to perform solubility calculations.

Acknowledgment. This research was supported by the Grant Agency of the Academy of Sciences of the Czech Republic

(grant IAA4072309), by the National Research Program "Information Society" (project 1ET400720507), by the National Research Council of Canada (grant OGP1041), and by the SHARCNET computing facility of the University of Guelph.

References and Notes

(1) McQuarrie, D. A.; Rock, P. A. *General Chemistry*, 3rd ed.; Freeman: New York, 1991.
(2) Sandler, S. I. *Chemical and Engineering Thermodynamics*, 3rd ed.; Wiley: New York, 1999.
(3) Cui, S. T.; Harris, J. G. *J. Phys. Chem.* **1995**, *99*, 2900.
(4) Ferrario, M.; Ciccotti, G.; Cartailler, T.; Spohr, E.; Turq, P. *J. Chem. Phys.* **2002**, *117*, 4947.
(5) Meijer, E. J.; Frenkel, D. *J. Chem. Phys.* **1990**, *92*, 7570.
(6) Frenkel, D.; Smit, B. *Understanding Molecular Simulation: From Algorithms to Applications*; Academic Press: London, 2002.
(7) Allen, M. P.; Tildesley, D. J. *Computer Simulation of Liquids*; Clarendon Press: Oxford, 1987.
(8) Orkoulas, G.; Panagiotopoulos, A. Z. *J. Chem. Phys.* **1994**, *101*, 1452.
(9) Orkoulas, G.; Panagiotopoulos, A. Z. *Fluid Phase Equilib.* **1993**, *83*, 223.
(10) Widom, B. *J. Chem. Phys.* **1963**, *39*, 2802.
(11) Lyubartsev, A. P.; Martsinovskii, A. A.; Shevkunov, S. V.; Vorontsov-Velyaminov, P. N. *J. Chem. Phys.* **1992**, *96*, 1776.
(12) Nezbeda, I.; Kolafa, J. *Mol. Simul.* **1991**, *5*, 391.
(13) Lyubartsev, A. P.; Forrisdahl, O. K.; Laaksonen, A. *J. Chem. Phys.* **1998**, *108*, 227.
(14) Panagiotopoulos, A. Z. *Fluid Phase Equilib.* **1992**, *76*, 97.
(15) Caillol, J. M. *J. Chem. Phys.* **1993**, *99*, 8953.
(16) Caillol, J. M. *J. Chem. Phys.* **1994**, *100*, 2161.
(17) Torrie, G. M.; Valleau, J. P. *Chem. Phys. Lett.* **1974**, *28*, 578.
(18) Torrie, G. M.; Valleau, J. P. *J. Comput. Phys.* **1977**, *23*, 187.
(19) Çagin, T.; Pettitt, B. M. *Mol. Simul.* **1991**, *6*, 5.
(20) Çagin, T.; Pettitt, B. M. *Mol. Phys.* **1991**, *72*, 169.
(21) Ji, J.; Çagin, T.; Pettitt, B. M. *J. Chem. Phys.* **1992**, *96*, 1333.
(22) Weerasinghe, S.; Pettitt, B. M. *Mol. Phys.* **1994**, *82*, 897.
(23) Lynch, G. C.; Pettitt, B. M. *J. Chem. Phys.* **1997**, *107*, 8594.
(24) Lo, C.; Palmer, B. *J. Chem. Phys.* **1995**, *102*, 925.
(25) Shroll, R. M.; Smith, D. E. *J. Chem. Phys.* **1999**, *110*, 8295.
(26) Shroll, R. M.; Smith, D. E. *J. Chem. Phys.* **1999**, *111*, 9025.
(27) Boinepalli, S.; Attard, P. *J. Chem. Phys.* **2004**, *119*, 12769.
(28) Escobedo, F. A.; de Pablo, J. J. *J. Chem. Phys.* **1996**, *105*, 4391.
(29) Banaszak, B. J.; Faller, R.; de Pablo, J. J. *J. Chem. Phys.* **2004**, *120*, 11304.
(30) Escobedo, F. A.; de Pablo, J. J. *J. Chem. Phys.* **1995**, *103*, 2703.
(31) Wilding, N. B.; Müller, M. *J. Chem. Phys.* **1994**, *101*, 4324.
(32) Åberg, K. M.; Lyubartsev, A. P.; Jacobsson, S. P.; Laaksonen, A. *J. Chem. Phys.* **2004**, *120*, 3770.
(33) Berendsen, H. J. C.; Grigera, J. R.; Straatsma, T. P. *J. Phys. Chem.* **1987**, *91*, 6269.
(34) Smith, D. E.; Dang, L. X. *J. Chem. Phys.* **1994**, *100*, 3757.
(35) Uchida, H.; Matsuoka, M. *Fluid Phase Equilib.* **2004**, *219*, 49.
(36) Brodholt, J. P. *Chem. Geol.* **1998**, *151*, 11.
(37) Beutler, T. C.; Mark, A. E.; van Schaik, R. C.; Gerber, P. R.; van Gunsteren, W. F. *Chem. Phys. Lett.* **1994**, *222*, 529.
(38) Andersen, H. C. *J. Chem. Phys.* **1980**, *72*, 2384.
(39) Berendsen, H. J. C.; Postma, J. P. M.; van Gunsteren, W. F.; DiNola, A.; Haak, J. R. *J. Chem. Phys.* **1984**, *81*, 3684.
(40) Beutler, T. C.; van Gunsteren, W. F. *Mol. Simul.* **1994**, *14*, 21.
(41) Lide, D. R. *CRC Handbook of Chemistry and Physics*; CRC Press: Boca Raton, FL, 1999.
(42) Chase, M., Jr. NIST-JANAF Thermochemical Tables. *J. Phys. Chem. Ref. Data, Monogr.* **1998**, *9*.
(43) Nezbeda, I.; Kolafa, J. *Mol. Simul.* **1995**, *14*, 153.
(44) Lísal, M.; Budinský, R.; Vacek, V. *Fluid Phase Equilib.* **1997**, *135*, 193.
(45) Vörtler, H. L.; Smith, W. R. *J. Chem. Phys.* **2000**, *112*, 5168.
(46) Haar, L.; Gallagher, J. S.; Kell, G. S. *NBS/NRC Steam Tables*; Hemisphere: Bristol, PA, 1984.
(47) Archer, D. G. *J. Phys. Chem. Ref. Data* **1992**, *21*, 793.